Quantum depinning of a domain wall in a magnetic field

Gwang-Hee Kim*
Department of Physics, Sejong University, Seoul 143-747, Korea
(Received 3 June 1998)

We investigate the quantum tunneling of a domain wall placed in a magnetic field at an arbitrary angle. Using classical soliton solutions, we derive a domain wall mass which depends on the magnetic field and find that the tunneling time and the crossover temperature strongly depend on the direction of the magnetic field. The results are also discussed at finite temperature. [S0163-1829(98)09641-6]

I. INTRODUCTION

In recent years, small magnetic particles have emerged as good candidates to display quantum behavior at a macroscopic scale.[1] One such system is nonuniform magnetic structure exhibiting a domain wall which is a soliton connecting two stable spin configurations separated by an energy barrier associated with magnetocrystalline anisotropy. In general, a domain wall is pinned by an impurity, lowering the anisotropy energy locally.[2] At finite temperature, there is a jumping of a domain wall induced by thermal fluctuations whose rate is proportional to $\exp(-U/k_BT)$ where U is the height of energy barrier related to the pinning energy.[3] At a temperature low enough to neglect the thermal activation, depinning of a domain wall may occur due to quantum tunneling by applying an external magnetic field. In order for a system to be a good example for quantum tunneling, the energy barrier through which it tunnels should be low and narrow, and the effective mass of the system be not too large, in which the tunneling rate becomes large enough for observing quantum tunneling of a domain wall (QTDW) involving $\sim 10^4$ spins. In this situation, the magnetic field is a good physical quantity to control the height and width of the barrier and the effective mass of the system. For the dynamical process, it is also important to consider the effect of the environments on the quantum tunneling rate caused by the coupling between the domain wall and magnons,[4,5] photons,[5] phonons,[4–6] nuclear spins,[7,8] eddy current, and Stoner excitations.[9] Even though some of them are an unsuspected influence on the quantum dynamics depending on the situation, many studies have shown that they are not strong enough to make QTDW unobservable.

Experiments which indicate the possible presence of tunneling of a domain wall have been reported. By measuring the electrical resistance of Ni wire with diameters between 20 and 40 nm, Hong and Giordano[10] studied the motion of magnetic domain walls and observed a flattening of the temperature dependence of the mean switching field and a saturation of the width of the escape field distribution below ~ 5 K. Even though they proposed that a domain wall escapes from its pinning sites by QTDW below ~ 5 K, their measurements raise several questions, among them whether the crossover temperature from thermally activated to quantum-mechanical decay is two or three orders of magnitude higher than the one predicted by current theories.[1] For the present it is not easy to perform a direct comparison between theoretical and experimental results.

A few theoretical studies of QTDW have been around for some time. Egami[11] gave a theoretical suggestion that the temperature-independent magnetic aftereffects observed at low temperature by Barbara and collaborators[12] might originate from the quantum diffusion of domain walls. However, his idea is only applicable to an extremely narrow wall whose width is of the order of the lattice constant and pinned by the crystal potential itself, which is contrary to typical walls having a thickness of ~ 100 Å and being pinned by an impurity. Even though several workers[13] suggested the tunneling of a domain wall by using the WKB method, QTDW did not receive wider attention until Stamp[4] investigated QTDW based on the Heisenberg model with a uniaxial anisotropy. By using a classical solution of the plane domain wall coupled to a point defect, he estimated the tunneling rate and contributions of magnons and phonons in terms of the coercive field, saturation magnetization, exchange, and anisotropy constants. Later, Chudnovsky, Iglesias, and Stamp[5] (CIS) developed a formulation of the problem which takes the curvature effects of a domain wall into consideration, and confirmed Stamp's work that the quantum tunneling of a domain wall may reveal itself at a macroscopic level. Besides the magnon and phonon studied by Stamp they briefly touched the effects of conduction electrons, photons, and the mobility of the domain wall. Since then, QTDW has been the subject of considerable theoretical interest. Among them, recently, Braun, Kyriakidis, and Loss[14] (BKL) found that the WKB exponent and the crossover temperature are of different functional forms than that found by CIS and the sources for these discrepancies are different soliton mass and functional dependence of the pinning potential on the coercivity.

Up to now theoretical studies for QTDW were confined to the condition that the magnetic field be applied in the opposite direction to the initial easy axis. In this work we will extend the previous considerations to a system with a magnetic field applied at some angle to the easy axis of magnetization. We will show that the WKB exponent depends on θ_H via $(1+\nu \tan \theta_H)^{1/2}$ and the crossover temperature on θ_H via $(1+\nu \tan \theta_H)^{-1/2}$ where ν will be discussed later. It implies that no tunneling is expected when the field is perpendicular to the easy axis. Also, we will present numerical results for the WKB exponent below the crossover temperature and discuss the thermal correction to the quantum tunneling rate.

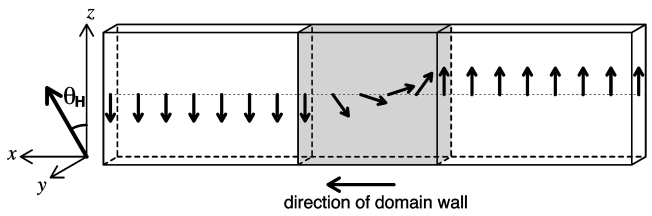

FIG. 1. A configuration of magnetization is shown in a thin long slab geometry where the wall plane is parallel to the easy axis (z) and the spin configuration spatially varies along in the x direction.

This paper is organized as follows. In Sec. II, we briefly discuss the domain wall dynamics for a ferromagnet by using the classical equation of motion. Applying an external magnetic field with a general direction (θ_H), we derive the effective domain wall mass which includes the field direction. In Sec. III, we perform the approximation of the potential in the small ϵ limit and find the expression which shows the explicit dependence of the physical parameters for the general form of the potential. Within the instanton approach, we obtain the θ_H dependence of the WKB exponent at $T=0$ for a specific pinning potential and estimate its magnitude for various magnetic materials.[14] These considerations will be extended to finite temperature in which the quantum and thermal fluctuation coexist. In Sec. IV, we numerically present the θ_H dependence of the tunneling time and the crossover temperature for the materials considered in Sec. III, and give the validity of the results derived near a classical depinning field.

II. FORMULATION OF THE PROBLEM

In this section, we consider the domain wall of the slab geometry, as shown in Fig. 1. We work with the systems by assuming that the domain wall thickness λ is sufficiently larger than the lattice constant a between spins in which a continuum approximation for the magnetization $\mathbf{M}$ is valid. Since the phenomena considered occur at a temperature far below the Curie temperature, the magnitude of the magnetization M_0 is constant. However, its direction $\hat{M}$ can change depending on the energy which is composed of the magnetic anisotropy energy, the exchange energy, and the demagnetization energy. As we introduce the angles θ and ϕ for the direction of $\mathbf{M}$ in the spherical coordinate system, the dynamics of $\hat{M}$ is determined by the least-action trajectory of the action

$$S[\mathbf{M}(\mathbf{r},t)]=\int\left\{\frac{M_0}{\gamma}[\cos\,\theta(\mathbf{r},t)-1]\,\frac{d\phi(\mathbf{r},t)}{dt}+E[\mathbf{M}(\mathbf{r},t)]\right\}dtd^3\mathbf{r}, \tag{1}$$

whose classical trajectory satisfies the well-known Landau-Lifshitz equation[15]

$$\frac{d\mathbf{M}}{dt}=-\gamma\mathbf{M}\times\frac{\delta E}{\delta\mathbf{M}}, \tag{2}$$

where $\gamma=g\mu_B/\hbar$ is the gyromagnetic factor. Here we note that the first term of the integrand in Eq. (1) has no classical analog which is called the Wess-Zumino term of the spin system[16] and whose phase space is the $(1\oplus1)$-dimensional space with the Poisson bracket relations of the spin angular momentum.[17]

For our study of the dynamics of $\hat{M}$ we take the biaxial symmetry whose magnetic anisotropy energy density is given by

$$E_a=-K_{\|}\hat{M}_z^2+K_{\perp,a}\hat{M}_y^2, \tag{3}$$

where $K_{\|}$ and $K_{\perp,a}$ are the parallel and transverse anisotropy constants. The easy axis is represented by $\pm\hat{M}_z$ and the easy plane is perpendicular to $\hat{M}_y$. Since the exchange energy density is expressed as $E_{\rm ex}=(C/2)(\nabla\hat{M})^2$ where C is an exchange constant, the energy density in the action (1) is given by

$$E[\theta(\mathbf{r},t),\phi(\mathbf{r},t)]=K_{\|}\sin^2\theta+K_{\perp}\sin^2\phi\sin^2\theta+\frac{1}{2}C[(\nabla\theta)^2+(\nabla\phi)^2\sin^2\theta], \tag{4}$$

where $E\equiv E_a+E_{\rm ex}+K_{\|}$ to make $E(\theta,\phi)$ zero at the easy axis, $K_{\perp}\equiv K_{\perp,a}+2\pi M_0^2$, and $2\pi M_0^2$ comes from the demagnetization energy for the slab geometry.

Following the analysis discussed in Ref. 14, for the sample with width $w<\pi\sqrt{C/2K_{\perp}}$ we can treat the system as quasi-one-dimensional. The domain wall corresponding to the energy density is perpendicular to the x axis, where the magnetization rotates in the easy plane (xz plane) and changes in the x axis. The wall position is centered at Q along the x axis. From Eq. (2) the soliton solution which describes the motion of the domain wall is given by

$$\theta_s(x-Q)=2\arctan\exp\left(\frac{x-Q}{\lambda}\right), \tag{5}$$

$$\dot{Q}=kv_0\frac{\sin\phi_s\cos\,\phi_s}{\sqrt{1+k\,\sin^2\phi_s}}, \tag{6}$$

where $k=K_{\perp}/K_{\|}$ and $v_0=\gamma\sqrt{2CK_{\|}}/M_0$. We note here that $\theta_s\to0\ (\pi)$ at $t\to\infty\ (-\infty)$ for a given spatial position x. The width of the wall is given by

$$\lambda=\frac{\lambda_0}{\sqrt{1+k\,\sin^2\phi_s}}, \tag{7}$$

where $\lambda_0=\sqrt{C/2K_{\|}}$ is the width of the static wall which represents a compromise between exchange and anisotropy energy. Assuming that $\dot{Q}$ is much smaller than the Walker critical velocity $v_0(\sqrt{1+k}-1)$,[2] the components of the magnetization are approximately given by

$$\hat{M}_x\simeq\mathrm{sech}\left(\frac{x-Q}{\lambda}\right)\left[1-\frac{1}{2}\left(\frac{\dot{Q}}{kv_0}\right)^2\right], \tag{8}$$

$$\hat{M}_y\simeq\mathrm{sech}\left(\frac{x-Q}{\lambda}\right)\left(\frac{\dot{Q}}{kv_0}\right), \tag{9}$$

$$\hat{M}_z \simeq \tanh\left(\frac{x-Q}{\lambda}\right), \tag{10}$$

and the corresponding energy becomes, from Eq. (4),

$$\int d^3\mathbf{r} E[\theta_s(\mathbf{r},t),\phi_s(\mathbf{r},t)] \simeq 2A_w\sqrt{2CK_\parallel} + \frac{1}{2}M\dot{Q}^2, \tag{11}$$

with the wall mass

$$M = A_w \frac{M_0^2}{\gamma^2 K_\perp}\sqrt{\frac{2K_\parallel}{C}}, \tag{12}$$

where A_w is the cross sectional area of the sample. As is noted in Eqs. (8), (9), and (10) a static domain wall only rotates in the easy plane. However, as it moves, the spins precess and a component of the magnetization out of the plane, $\hat{M}_y$, appears with $\hat{M}_y \propto \dot{Q}$ in Eq. (9). Thus, the inertial term in Eq. (11) is closely related to the precession of the spins. If defects are present in the samples, they can pin the domain wall. Assuming that the radius R corresponding to the defect volume is much smaller than the wall thickness λ, the wall is pinned by a potential form[4]

$$V_p(Q) = -V_0 \mathrm{sech}^2(Q/\lambda_0), \tag{13}$$

with V_0 proportional to the volume of the defect, where we have replaced λ by λ_0 and neglected the higher order of $O(V_0/E_0)$ with $E_0 = 2A_w\sqrt{2CK_\parallel}$. Also, assuming that a concentration of defects is small, the pinning energies become small, in which the radius of curvature of the wall is much larger than λ. Since it is shown[5,18] that weak curvature has very little effect on wall tunneling, the wall can be assumed to be flat and remained flat during the tunneling process.

If we now apply an external magnetic field in the xz plane, its energy is written as

$$\begin{aligned}\int d^3\mathbf{r} E_H[\mathbf{M}(\mathbf{r},t)] &= -A_w\int dx(M_0H_z\hat{M}_z + M_0H_x\hat{M}_x)\\ &\simeq -2A_wM_0H_zQ + \pi A_w\lambda M_0H_x\\ &\quad\times\left(\frac{k+1}{2}\right)\left(\frac{\dot{Q}}{kv_0}\right)^2,\end{aligned} \tag{14}$$

where Eqs. (8) and (10) were inserted. Thus, from Eqs. (11), (13), and (14) we obtain the total energy for the wall:

$$\int d^3\mathbf{r}(E+E_H) = \frac{1}{2}M_{\mathrm{eff}}\dot{Q}^2 + V_p(Q) - h_zQ, \tag{15}$$

where $M_{\mathrm{eff}} = M + \pi A_w\lambda_0 M_0 H_x(k+1)/(kv_0)^2$ and $h_z = 2A_wM_0H_z$.

III. QUANTUM TUNNELING OF THE DOMAIN WALL

Before we get into a discussion of the specific form of the pinning potential such as Eq. (13), we consider an arbitrary pinning potential which might be useful for a situation like many random impurities. Since the external magnetic field brings the system into a metastable state, the domain wall can tunnel out of the potential. As the magnetic field continues to increase, the metastable minimum can disappear and the domain wall moves classically. This critical magnetic field is called a classical depinning field (CDF). In order to make the potential barrier small and narrow which is the optimum condition for the observability of tunneling events as we shall see, we concentrate ourselves on the neighborhood of the CDF. In this situation, let us define the potential to be

$$U_1(Q) = V_p(Q) - h_zQ - [V_p(Q_0) - h_zQ_0], \tag{16}$$

where $(Q_0,0)$ is the metastable point of $U_1(Q)$. Expanding the pinning potential $V_p(Q)$ around $Q=Q_i$ which is the Q coordinate of the inflection point of $V_p(Q)$, we obtain an approximate form of the potential given by[19]

$$U(q) \simeq [V_p'(Q_i) - h_z](q-q_0) + \frac{V_p^{(n)}(Q_i)}{n!}(q^n - q_0^n), \tag{17}$$

where $U(q) \equiv U_1(Q)$, $q = Q - Q_i$, $q_0 = Q_0 - Q_i (<0)$, and the higher-order terms are neglected. Noting that $V_p^{(2)}(Q_i) = 0$, n is greater than 2. In order that $U(q)$ have a metastable state, we need $V_p'(Q_i) > h_z$ and $V_p^{(n)}(Q_i) < 0$, and n should be odd. Since the local minimum vanishes for $h_z \geq V_p'(Q_i)$ in Eq. (17), $V_p'(Q_i)$ becomes the CDF. Denoting $V_p'(Q_i)$ to be h_z^c, from Eq. (17) the metastable point q_0 is given by

$$q_0 = -\left[\frac{(n-1)!}{|V_p^{(n)}(Q_i)|}h_z^c\epsilon\right]^{1/(n-1)}, \tag{18}$$

where $\epsilon = 1 - h_z/h_z^c = 1 - h/h_c$ and $h_z^c [= V_p'(Q_i)] = h_c\cos\theta_H$. In a magnetic field lower than CDF, the domain wall can make a tunnel through the potential barrier. Then, according to the standard instanton method ($\tau \equiv it$), we can obtain the tunneling rate given by

$$\Gamma = C_0\sqrt{\frac{B}{2\pi}}\,\omega_t \exp(-B), \tag{19}$$

where ω_t is a characteristic tunneling frequency which is of the order of the barrier frequency ω_0 and B ($= S_{\mathrm{cl}}/\hbar$) determined by the classical trajectory from the Euclidean action

$$S_E = \int_{-\beta\hbar/2}^{\beta\hbar/2} d\tau\left[\frac{1}{2}M_{\mathrm{eff}}\left(\frac{dq}{d\tau}\right)^2 + U(q)\right], \tag{20}$$

with $\beta = 1/k_BT$. In Eq. (19), C_0 is the preexpotential factor which stems from the quantum fluctuations around the least-action trajectory.

Applying the scale transformations to the action (20), we obtain

$$\begin{aligned}S_E &= \left[\frac{(n-1)!}{|V_p^{(n)}(Q_i)|}\right]^{3/2(n-1)}(h_c^z\epsilon)^{(n+2)/2(n-1)}\sqrt{M_{\mathrm{eff}}}\\ &\quad\times\int_{-\Lambda/2}^{\Lambda/2} d\tilde{\tau}\left[\frac{1}{2}\left(\frac{d\tilde{q}}{d\tilde{\tau}}\right)^2 + \tilde{U}(\tilde{q})\right],\end{aligned} \tag{21}$$

where $q = -q_0\tilde{q}$, $\tau = \tilde{\tau}/\tau_0$, and $\Lambda = \beta\hbar\tau_0$ with

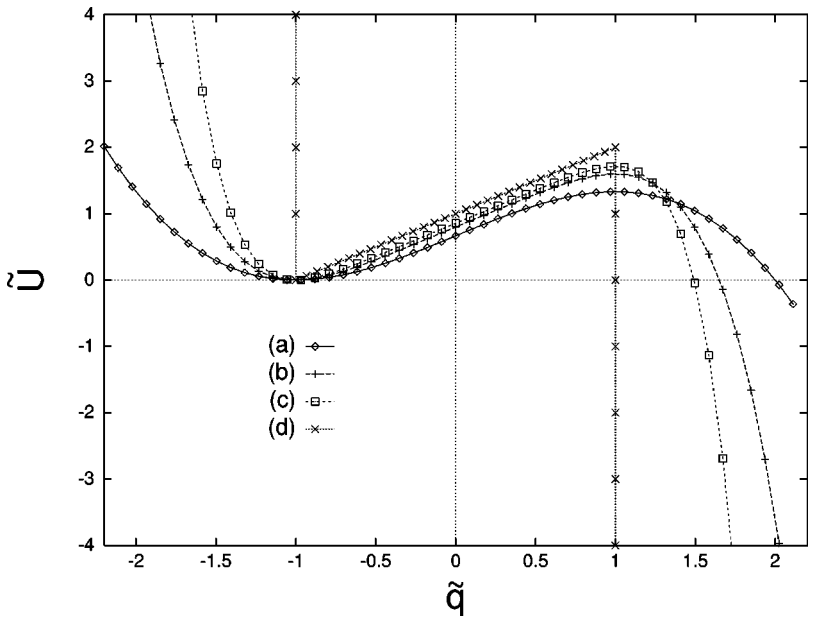

FIG. 2. The $\tilde{q}$ dependence of the scaled potential $\tilde{U}(\tilde{q})$ for different values of n, where $n=3$ (a), 5 (b), 7 (c), and ∞ (d). Note that $(-1,0)$ and $(1,\ 2-2/n)$ are the metastable point and the barrier, respectively.

$$\tau_0=\frac{(h_c^z\epsilon)^{(n-2)/2(n-1)}}{\sqrt{M_{\rm eff}}}\left[\frac{|V_p^{(n)}(Q_i)|}{(n-1)!}\right]^{1/2(n-1)}, \tag{22}$$

and $\tilde{U}(\tilde{q})=\tilde{q}+1-(\tilde{q}^n+1)/n$. As is shown in Fig. 2, the $\tilde{q}$ position of the barrier is 1 which is independent of n, the height of barrier $\tilde{U}_m=2(1-1/n)$, and the scaled barrier frequency $\tilde{\omega}_0[=\sqrt{-\tilde{U}''(\tilde{q}_m)}]=(n-1)^{1/2}$ which characterizes the width of the top of the barrier frequency hindering the tunneling process. From Eq. (21) the extremal trajectory satisfies

$$\frac{d^2\tilde{q}}{d\tilde{\tau}^2}-(1-\tilde{q}^{n-1})=0, \tag{23}$$

with the periodic condition $\tilde{q}(\tilde{\tau})=\tilde{q}(\tilde{\tau}+\Lambda)$. From now on let us consider the specific pinning potential (13), in which $V^{(3)}(Q_i)$ is the first nonvanishing term in Eq. (17).

A. QTDW at zero temperature

With the boundary conditions $\tilde{q}(\pm\infty)=0$ and $\tilde{q}(0)=\tilde{q}_0$ at $T=0$ where $\tilde{q}_0$ is the exit point of the potential $\tilde{U}(\tilde{q})$, the solution of Eq. (23) for $n=3$ becomes

$$\tilde{q}(\tilde{\tau})=3\,\mathrm{sech}^2(\tilde{\tau}/\sqrt{2})-1. \tag{24}$$

The substitution of this solution into Eq. (21) with $n=3$ gives a simple formula for the WKB exponent B,

$$B(\theta_H)=B_0\sqrt{1+\nu\,\tan\,\theta_H}, \tag{25}$$

where

$$B_0=\frac{12\times 2^{3/4}}{5}\mu\epsilon^{5/4}, \tag{26}$$

$$\mu=\frac{A_w}{\gamma\hbar}\,M_0^{3/2}\sqrt{\frac{C}{K_\parallel K_\perp}}\,\sqrt{H_z^c}, \tag{27}$$

$$\nu=\frac{\pi}{4}M_0H_z^c\left(\frac{1}{K_\parallel}+\frac{1}{K_\perp}\right), \tag{28}$$

$$H_z^c\left(=\frac{h_z^c}{2A_wM_0}\right)=\frac{2\sqrt{6}}{9}\,\frac{V_0}{A_wM_0}\,\sqrt{\frac{K_\parallel}{C}}, \tag{29}$$

$$H_c=\frac{H_z^c}{\cos\,\theta_H}. \tag{30}$$

Up to the numerical factor the expression (25) can be obtained from the ratio of the barrier height U_m to the barrier frequency ω_e without knowing the explicit form of the bounce solution (24). By using the general form of the potential (17), the height of barrier and the barrier frequency which represents the frequency of small oscillations around the minimum of the inverted potential $-U(q)$ are given by

$$U_0=2\left[\frac{(n-1)!}{|V_p^{(n)}(Q_i)|}\right]^{1/(n-1)}(h_c^z\epsilon)^{n/(n-1)}\left(1-\frac{1}{n}\right), \tag{31}$$

$$\omega_e=\frac{[(n-1)!]^{(n-2)/2(n-1)}}{[(n-2)!]^{1/2}}\times\frac{(h_c^z\epsilon)^{(n-2)/2(n-1)}|V_p^{(n)}(Q_i)|^{1/2(n-1)}}{\sqrt{M_{\rm eff}}}. \tag{32}$$

Thus, with the help of Eq. (13), $M_{\rm eff}$, and h_z in Eq. (15), its ratio for $n=3$ becomes

$$\frac{U_0}{\hbar\,\omega_e}=\frac{5}{36}B(\theta_H), \tag{33}$$

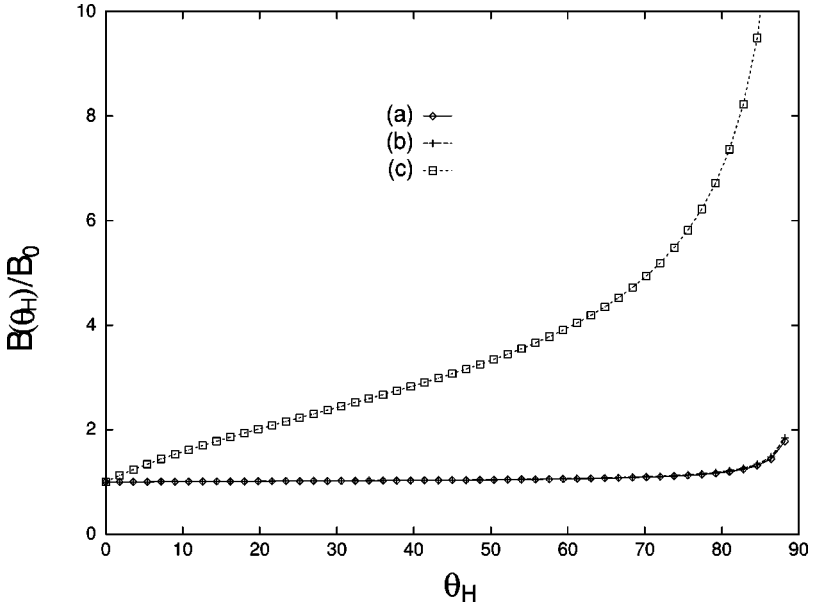

FIG. 3. The θ_H dependence of the relative WKB exponent $B(\theta_H)/B_0$ for the samples (a) YIG, (b) Ni, and (c) $SrRuO_3$.

where 5/36 is a typical numerical constant for linear- (or quadratic-) plus-cubic potential.[20]

The angular dependence of B is plotted in Fig. 3 for ferromagnetic samples of yttrium iron garnet (YIG), Ni, and $SrRuO_3$ by using the physical values given in Table I. In these materials it rises sharply as θ_H approaches $\pi/2$ in accordance with the fact that at $\theta_H=\pi/2$ the potential for Q created by impurities is not deformed by the magnetic field and the position of the domain wall at the pinning center is not metastable any more. In YIG and Ni the behavior of the ratio $B(\theta_H)/B_0$ is almost flat for θ_H not close to $\pi/2$. However, in $SrRuO_3$ it has a strong dependence on the orientation of the field because of a large ν mainly originating from a larger coercivity H_z^c compared with the coercivities for YIG and Ni. It would therefore be interesting to study the angular dependence of the WKB exponent in $SrRuO_3$.

In order to obtain the complete form of the tunneling rate Γ, we need to calculate the preexponential factor C_0 in Eq. (19) which comes from the fluctuation about the least-action trajectory. Since the potential is of the form $q-q^3$ in our case, the preexponential factor becomes $C_0=4\sqrt{15}$, which is the same as the result in the potential of the form q^2-q^3.[21] From the bounce (24) and the scaling parameter (22) for $n=3$ the angular dependence of the characteristic tunneling frequency is represented as $\omega_t(\theta_H)=\omega_t^0/\sqrt{1+\nu\tan\theta_H}$ with $\omega_t^0=\gamma(2\epsilon)^{1/4}(H_z^cK_\perp/M_0)^{1/2}$. Writing the tunneling rate as $\Gamma=A\exp(-B)$, A depends on the orientation of the magnetic field through $(1+\nu\tan\theta_H)^{-1/4}$. Noting the θ_H behavior of B and A, the tunneling rate decreases as θ_H increases.

B. QTDW at finite temperature

In this case the classical trajectory $\tilde{q}_{\rm cl}(\tilde{\tau})$ which minimizes the action satisfies Eq. (23) with period Λ. The periodic solutions are $\tilde{q}_0(=1)$ and $\tilde{q}(\tilde{\tau})$, determined by

$$\frac{1}{2}\left(\frac{d\tilde{q}}{d\tilde{\tau}}\right)^2=\tilde{q}+1-\frac{\tilde{q}^3+1}{3}-\tilde{E}(\Lambda), \tag{34}$$

where $\tilde{E}$ is determined by the condition that the period of the motion is equal to Λ. For the constant solution $\tilde{q}_0$ the classical action becomes, from Eqs. (21), (22), and (31),

$$S_E^{\rm cl}=S_0=\beta\hbar U_0, \tag{35}$$

and the escape rate

$$\Gamma_0\propto\exp(-S_0/\hbar)=\exp(-U_0/k_BT), \tag{36}$$

which is the Boltzmann formula representing a pure thermal activation. In the case that the solution of Eq. (34) is a periodic function with period $\Lambda=\Lambda(T)$, $\tilde{q}_{\rm cl}(\tilde{\tau})$ can be expanded into a Fourier series:

TABLE I. Saturation magnetization M_0, easy-axis anisotropy constant $K_\parallel$, shape anisotropy $K_\perp\simeq 2\pi M_0^2$ for a thin film, exchange constant C, wall width λ_0, and coercivity H_z^c taken from Ref. 14 for various materials and the corresponding parameter ν. Also, the WKB exponent B_0, the characteristic frequency ω_t^0, the tunneling time Γ_0^{-1}, and the crossover temperature $T_c(\theta_H=0)$ are obtained from a given value of ϵ.

	M_0 [Oe]	$K_\parallel$ [10^5 erg/cm^3]	$K_\perp$ [10^5 erg/cm^3]	C [10^{-6} erg/cm^3]	λ_0 [Å]	H_z^c [Oe]	ν	ϵ [10^{-3}]	B_0	ω_t^0 [10^8/sec]	Γ_0^{-1} [sec]	$T_c(0)$ [mK]
YIG	196	0.25	2.4	0.86	414	10	0.068	5	30	6.20	528	1.50
Ni	508	8	16	2	112	100	0.075	4	31	29.7	385	7.18
$SrRuO_3$	159	20	1.6	0.046	11	10^4	8.43	5	22	222	5.46×10^{-3}	42.9

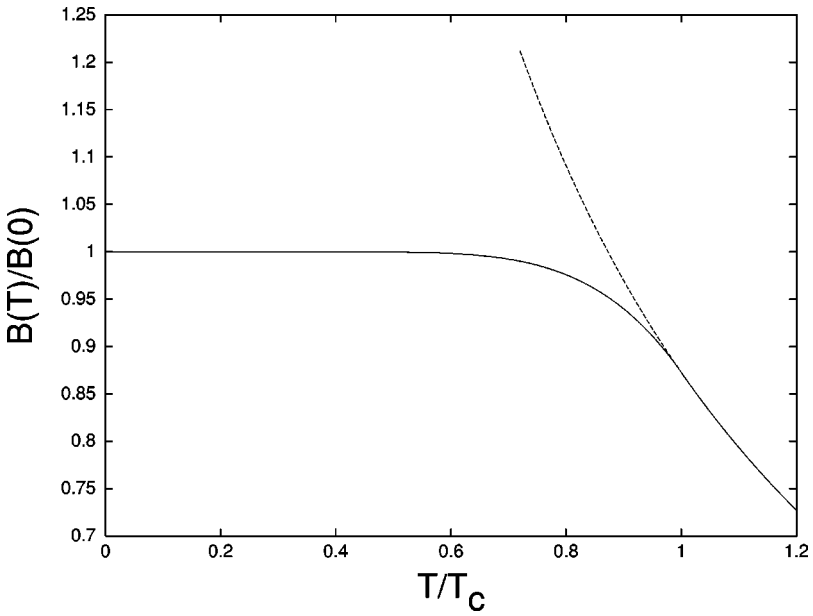

FIG. 4. Temperature dependence of the WKB exponent: $B(T)/B(0)$ vs T/T_c. The solid line is obtained from the numerical integration of Eq. (21) by using the bounce solution of Eq. (34) and dotted line is the Boltzmann formula for comparison.

$$\tilde{q}_{\rm cl}(\tilde{\tau})=\sum_{n=-\infty}^{\infty}\tilde{q}_n\exp(i\tilde{\omega}_n\tilde{\tau}), \tag{37}$$

where $\tilde{q}_n$'s are Fourier coefficients and $\tilde{\omega}_n=2\pi n/\Lambda$. The differential equation (23) for $\tilde{q}_{\rm cl}(\tilde{\tau})$ is then transformed into

$$-\tilde{\omega}_n^2\tilde{q}_n-\delta_{n,0}+\sum_{n=-\infty}^{\infty}\tilde{q}_{n-m}\tilde{q}_m=0, \tag{38}$$

and the integral part of the action (21) in the $\tilde{\tau}$ space is expressed as

$$I\equiv\Lambda\sum_{n=-\infty}^{\infty}\left[\left(\tilde{q}_n+\frac{2}{3}\right)\delta_{n,0}+\frac{1}{2}\tilde{q}_n^2\tilde{\omega}_n^2-\frac{1}{3}\sum_{m=-\infty}^{\infty}\tilde{q}_n\tilde{q}_{n-m}\tilde{q}_m\right], \tag{39}$$

which further reduces to

$$I=\Lambda\sum_{n=-\infty}^{\infty}\left[\frac{2}{3}(\tilde{q}_n+1)\delta_{n,0}+\frac{1}{6}\tilde{q}_n^2\tilde{\omega}_n^2\right], \tag{40}$$

by making use of the relationship given by Eq. (38).

Now let us define T_c to be the temperature at which the periodic solution $\tilde{q}_{\rm cl}(\tilde{\tau})$ of Eq. (34) approaches the constant solutions $\tilde{q}_0$. In the limit of $T\lesssim T_c$, the thermal bounce $\tilde{q}_{\rm cl}(\tilde{\tau})$ oscillates around the bottom of the inverse potential $-\tilde{U}(\tilde{q})$. In this situation $\tilde{q}_0$ and $\tilde{q}_{\pm1}$ are dominant in the Fourier series (37) of the thermal bounce $\tilde{q}_{\rm cl}(\tilde{\tau})$, which is reduced to[22,23]

$$\tilde{q}_{\rm cl}(\tilde{\tau})=\tilde{q}_0+2\tilde{q}_1\cos(\tilde{\omega}_1\tilde{\tau}), \tag{41}$$

with $\tilde{q}_1(T_c)=0$. By using the fact that $\tilde{q}_0=1$ and $\tilde{q}_1=0$ at $T=T_c$ and solving Eq. (38), we can obtain the temperature dependence of two Fourier coefficients,

$$\tilde{q}_0=\left(\frac{T}{T_c}\right)^2,\quad \tilde{q}_1=\frac{1}{\sqrt{2}}\sqrt{1-\left(\frac{T}{T_c}\right)^4}, \tag{42}$$

and $\Lambda_c=\sqrt{2}\pi$ which leads to an expression for T_c:

$$T_c=\frac{T_c(0)}{\sqrt{1+\nu\tan\theta_H}}, \tag{43}$$

where

$$k_BT_c(0)=\frac{\hbar}{\sqrt{2}\pi}(2\epsilon)^{1/4}\sqrt{(\gamma H_z^c)\left(\frac{2\gamma K_\perp}{M_0}\right)}. \tag{44}$$

Substituting the coefficients (42) into the integral (40), the WKB exponent of Eq. (21) is approximately given by

$$\frac{S_E^{\rm min}}{\hbar}\approx\frac{U_0}{k_BT}\left[1-3\left(1-\frac{T}{T_c}\right)^2\right]. \tag{45}$$

The thermal action (45) should be compared with the action (35) of the constant path $\tilde{q}_0$ because the smallest of the two determines the actual escape rate of Eq. (19). Since $S_E^{\rm min}<S_0$, the functional integral for the decay is dominated by the thermal bounce for $T\lesssim T_c$. Hence T_c is the temperature in which quantum mechanics starts to make an effect on the WKB exponent, i.e., the crossover temperature from the thermal to the quantum regime. Also, we note that since the Boltzmann formula (36) derived from the constant path $\tilde{q}_{\rm cl}(\tilde{\tau})=\tilde{q}_0$ is valid above T_c, the thermal bounce degenerates into a constant path for $T\geqslant T_c$.

The bounce solution of Eq. (34) is found numerically in the entire range of temperatures $T\leqslant T_c$ and its numerical integration in Eq. (21), using this solution, gives us the WKB

TABLE II. Equivalent expressions for coefficient $V_p^{(3)}(Q_i)$ of the highest important term in Eq. (17), the attempt frequency ω_a around the metastable minimum, the barrier frequency ω_e, the bounce frequency ω_t, and the height of barrier U_0 for the given pinning potential (13), where $n=3$ and $Q_i=\lambda_0 \arctan(1/\sqrt{3})$. ω_t^0 and h_z^c are given in the text.

$V_p^{(3)}(Q_i)$	$\omega_a=\omega_e\ (=2\omega_t)$	U_0
$4h_c^z/\lambda_0^2$	$(2\lvert V_p^{(3)}(Q_i)\rvert h_c^z\epsilon)^{1/4}/\sqrt{M_{\rm eff}}$	$\frac{4\sqrt{2}}{3}(h_c^z\epsilon)^{3/2}/\lvert V_p^{(3)}(Q_i)\rvert^{1/2}$
$-\frac{32\sqrt{6}}{9}V_0(K_\parallel/C)^{3/2}$	$2\omega_t^0/\sqrt{1+\nu\ \tan\ \theta_H}$	$\frac{\sqrt{6}}{27}V_0\epsilon^{3/2}$

exponent. Figure 4 plots the ratio $B(T)/B(0)$ versus T/T_c, where the value of the integral part of the action (21) at $T=0$ is $24\sqrt{2}/5$ and $B(T_c)/B(0)=5\pi/18$. For $0\leqslant T\lesssim 0.6T_c$ $B(T)\simeq B(0)$, and the WKB exponent starts to deviate from the $B(0)$ at about $T\simeq 0.6T_c$ and continues to decrease until $T=T_c$.

We shall now consider the rate formula for a pure thermal activation regime (thermal hopping) and for temperatures beyond the crossover region but well below the pure classical escape regime (quantum corrections), where quantum corrections to the classical escape rate become increasingly important.[24] Above T_c the effect of quantum fluctuations on the rate emerges through the preexponential factor in which the rate is expressed as[25]

$$\Gamma=\frac{\omega_a}{2\pi}c_q\exp(-\beta U_0), \tag{46}$$

where ω_a and U_0 are given in Table II. Also, the factor c_q arising from fluctuations about the stationary trajectories $\tilde{q}(\tilde{\tau})=\pm 1$ is determined by carrying out the Gaussian integrals over the sets of amplitudes $\{\tilde{q}_n\}$ in the Fourier series and its resultant expression is then given by

$$c_q=\prod_{n=1}^{\infty}\frac{\omega_n^2+\omega_a^2}{\omega_n^2-\omega_e^2}, \tag{47}$$

where $\omega_n=2\pi n/\beta\hbar$ and ω_e is given in Table II. Using the infinite product representation of the sinh function,

$$\prod_{n=1}^{\infty}\frac{\omega_n^2}{\omega^2+\omega_n^2}=\frac{\beta\hbar\omega/2}{\sinh(\beta\hbar\omega/2)}, \tag{48}$$

we obtain the factor

$$c_q=\left(\frac{\omega_e}{\omega_a}\right)\frac{\sinh(\beta\hbar\omega_a/2)}{\sin(\beta\hbar\omega_e/2)}. \tag{49}$$

In the classical limit ($T\gg T_c$), the factor c_q approaches unity, so that

$$\Gamma=\frac{\omega_t^0}{\pi\sqrt{1+\nu\ \tan\ \theta_H}}\exp(-\beta U_0). \tag{50}$$

In the quantum correction regime the average energy is increased in the well and the effective height of barrier is reduced because a particle is thermally excited to the barrier, which leads to the enhancement of the escape rate. Taking

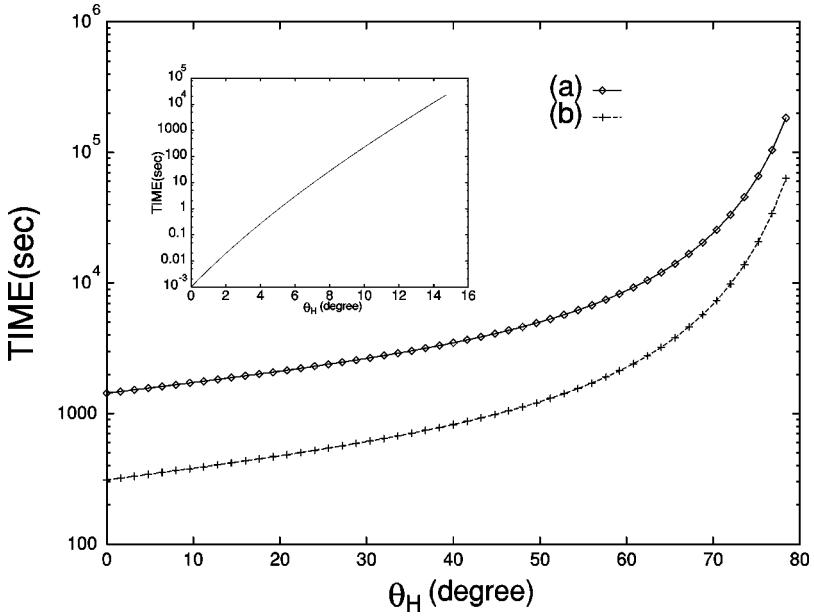

FIG. 5. The θ_H dependence of the tunneling time $\Gamma^{-1}(\theta_H)$ for the samples (a) YIG and (b) Ni. Inset: $\Gamma^{-1}(\theta_H)$ for $SrRuO_3$.

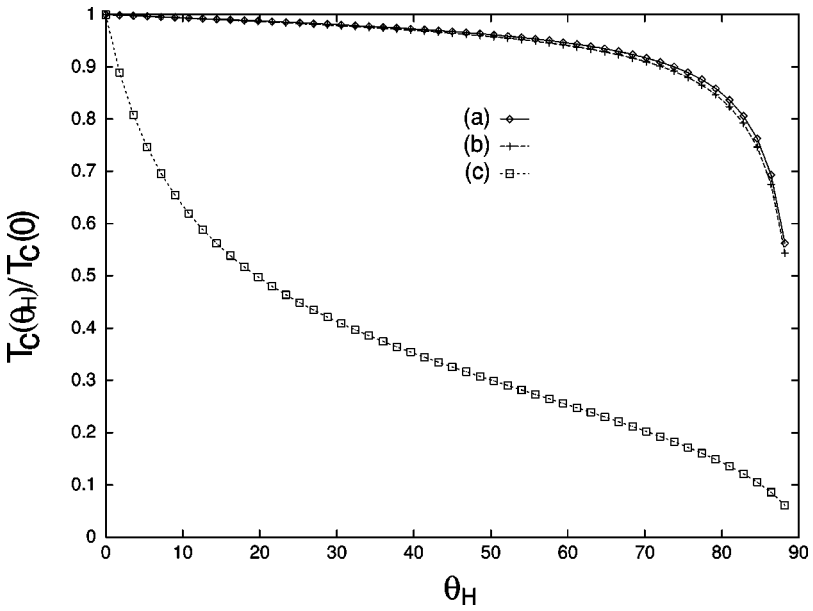

FIG. 6. The θ_H dependence of the relative crossover temperature $T_c(\theta_H)/T_c(0)$ for the samples (a) YIG, (b) Ni, and (c) $SrRuO_3$.

the factor (49) as the exponential of a sum of logarithms and expanding each logarithm in powers of $\beta\hbar$, its approximate form is given by

$$c_q \simeq \exp\left[\frac{1}{3}\left(\frac{\hbar\omega_t^0}{k_B T}\right)^2 \frac{1}{1+\nu\tan\theta_H}\right], \tag{51}$$

which indicates a thermally assisted quantum tunneling process.

IV. DISCUSSION AND CONCLUSIONS

In Fig. 5 we have illustrated the tunneling time with concrete number for various materials given in Table I. The typical angles expected to tunnel out of a potential within experimentally reasonable tunneling time $\Gamma^{-1}(\theta_H)$ are $0 \leqslant \theta_H < 90°$ for YIG and Ni, and $0 \leqslant \theta_H < 16°$ for $SrRuO_3$ in the case of $\epsilon \simeq O(10^{-3})$. The tunneling time changes more apparently in $SrRuO_3$ than in YIG and Ni.

By using Eq. (43), we obtain the angular dependence of the crossover temperature T_c, as is shown in Fig. 6. As θ_H increases, the crossover temperature decreases monotonically. As noted in this figure and in Table I, the shape of $T_c(\theta_H)/T_c(0)$ and the order of magnitude of $T_c(0)$ for YIG are the same as those for Ni. However, for $SrRuO_3$ they are strikingly different due to the large value of the parameter ν for $SrRuO_3$, as previously discussed in the WKB exponent. Thus, in order to obtain the angular dependence of T_c as well as the higher magnitude of $T_c(0)$ in QTDW, it would be more desirable to choose $SrRuO_3$ for future experiments.

In this paper we have considered the quantum depinning

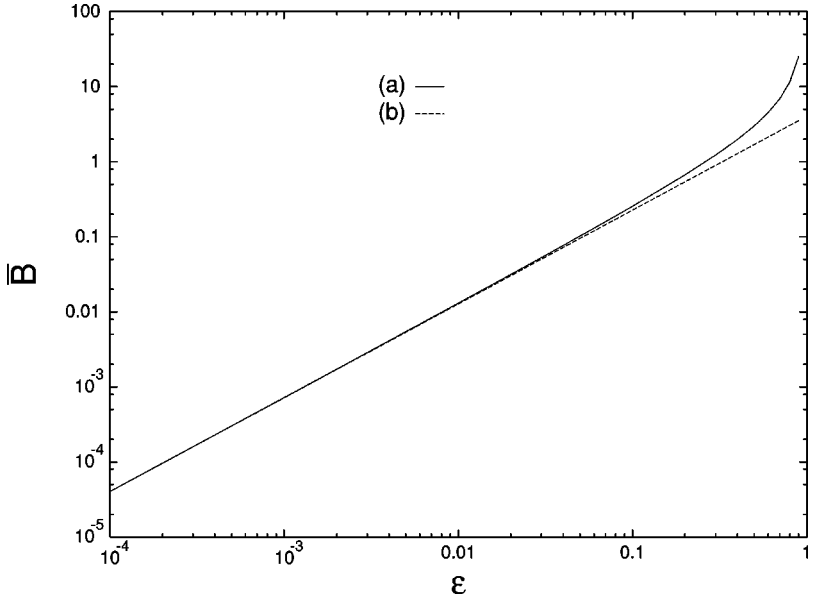

FIG. 7. The ϵ dependence of the scaled WKB, $\bar{B}(\equiv B/\mu)$, where (a) the numerical result from the exact potential (16) and (b) the approximate result (26) in the small ϵ limit.

of a domain wall placed at some angle with the magnetic field. In the limit of small ϵ the potential was expanded around the inflection point and the WKB exponent found for the general pinning potential up to a numerical constant. For the specific pinning potential we have obtained a magnetic field dependence of the WKB exponent, the oscillation frequency, the tunneling time, and the crossover temperature based on the instanton approach. Comparing the approximate WKB exponent with the exact numerical calculation, the limit of the applicability of the results is $\epsilon \lesssim 0.01$ which is shown in Fig. 7. At finite temperature we have discussed the thermal (quantum) correction to the quantum (thermal) escape rate. Finally, using the physical quantities taken from Table I, we have performed concrete estimations for the θ_H dependence of the WKB exponent and the crossover temperature for specific magnetic materials. As a good candidate for observing these behaviors experimentally, we have suggested a material with a large coercivity such as $SrRuO_3$ which gives a large ν.

ACKNOWLEDGMENTS

I am indebted to H. Fukuyama, D. S. Hwang, and H. C. Jeong for many useful discussions. This work was supported in part by the Basic Science Research Institute Program, Ministry of Education, Project No. BSRI-98-2415, and in part by the Non-Directed-Research-Fund, Korea Research Foundation, 1998.

*Electronic address: gkim@kunja.sejong.ac.kr

[1] L. Gunther and B. Barbara, *Quantum Tunneling of Magnetization-QTM '94* (Kluwer Academic, Dordrecht, 1995).
[2] A. P. Malozemoff and J. C. Slonczewski, *Magnetic Domain Walls in Bubble Materials* (Academic Press, New York, 1979).
[3] H. A. Kramers, Physica (Utrecht) **7**, 284 (1940).
[4] P. C. E. Stamp, Phys. Rev. Lett. **66**, 2802 (1991).
[5] E. M. Chudnovsky, O. Iglesias, and P. C. E. Stamp, Phys. Rev. B **46**, 5392 (1992).
[6] A. Garg and G.-H. Kim, Phys. Rev. Lett. **63**, 2512 (1989); Phys. Rev. B **43**, 712 (1991); H. Simanjuntak, J. Low Temp. Phys. **90**, 405 (1992).
[7] O. M. Dube and P. C. E. Stamp, J. Low Temp. Phys. **110**, 779 (1998).
[8] A. Garg, Phys. Rev. Lett. **70**, 1541 (1993); N. Prokofév and P. C. E. Stamp, J. Phys.: Condens. Matter **5**, L663 (1993); A. Garg (unpublished).
[9] G. Tatara and H. Fukuyama, Phys. Rev. Lett. **72**, 772 (1994); J. Phys. Soc. Jpn. **63**, 2538 (1994).
[10] K. Hong and N. Giordano, J. Magn. Magn. Mater. **151**, 396 (1995); J. Phys.: Condens. Matter **8**, L301 (1996).
[11] T. Egami, Phys. Status Solidi A **20**, 157 (1973); Phys. Status Solidi B **57**, 211 (1973).
[12] B. Barbara, G. Fillion, D. Gignoux, and R. Lemaire, Solid State Commun. **10**, 1149 (1972).
[13] J. A. Baldwin and F. Milstein, J. Appl. Phys. **45**, 4006 (1974); W. Riehemann and E. Nemback, *ibid.* **55**, 1081 (1983); **57**, 476 (1985).
[14] H.-B. Braun, J. Kyriakidis, and D. Loss, Phys. Rev. B **56**, 8129 (1997).
[15] V. G. Bar'yakhtar, M. V. Chetkin, B. A. Ivanov, and S. N. Gadetskii, *Dynamics of Topological Magnetic Solitons* (Springer-Verlag, Berlin, 1994); W. F. Brown, Jr., *Magnetostatic Principles in Ferromagnetism* (North-Holland, Amsterdam, 1962).
[16] *Geometric Phases in Physics A*, edited by A. Shapere and F. Wilczek (World Scientific, Singapore, 1989).
[17] G.-H. Kim and D. S. Hwang, Phys. Lett. A **241**, 223 (1998).
[18] P. C. E. Stamp, E. M. Chudnovsky, and B. Barbara, Int. J. Mod. Phys. B **6**, 1355 (1992).
[19] S. Nakaya and K. Hida, J. Phys. Soc. Jpn. **55**, 3768 (1986).
[20] A quadratic-plus-cubic potential is obtained by expanding the pinning potential around the metastable point $Q = Q_0$.
[21] A. O. Caldeira and A. J. Leggett, Ann. Phys. (N.Y.) **149**, 374 (1983); M.-C. Miguel and E. M. Chudnovsky, Phys. Rev. B **54**, 388 (1996); G.-H. Kim and D. S. Hwang, *ibid.* **55**, 8918 (1997).
[22] E. M. Chudnovsky, Phys. Rev. A **46**, 8011 (1992).
[23] G.-H. Kim, Phys. Rev. B **57**, 10 688 (1998).
[24] We have also performed calculations just above and below the crossover temperature which is called the crossover region. In this region the formulas are very complicated and so we just briefly discuss them. Since we have $\omega_1 = \omega_e$, equivalently, $\Lambda_c = \sqrt{2}\pi$ at the crossover temperature, the Gaussian integral diverges. Therefore, we cannot disregard terms of the third and higher order in the expansion about the constant paths. In this respect we need to extend the regular second-order action by terms up to the non-Gaussian terms in the action functional. Then, the quantum fluctuation displays a nonsingularity at $T = T_c$ and smears the transitions in the crossover region, in which the WKB exponent is of the form (45).
[25] U. Weiss, *Quantum Dissipative Systems* (World Scientific, Singapore, 1993).